



Frascati Physics Series Vol. nnn (2001), pp. 000-000

HEAVY QUARKS AT FIXED TARGET - Rio de Janeiro, Oct. 9-12, 2000

**REVIEW OF HEAVY-QUARK PRODUCTION AT  
FIXED-TARGET EXPERIMENTS**

Jeffrey A. Appel

*Fermilab, P.O. Box 500, Batavia, IL 60510, USA*

**ABSTRACT**

An increasingly large amount of quality fixed-target data on heavy-quark production at fixed-target energies is appearing. This data can provide information across a range of physics topics. The topics vary from investigations of QCD predictions to the understanding of the structure of hadrons. Recent results on neutrino, photon, and hadron production of charm and beauty will be reviewed in this context. The greatest insight will come from combining multiple measurements as they relate to the physics topics, and by ensuring that the parameters used in models are consistent with all the measurements. We have not yet really entered the time when this has been done for fixed-target measurements.

## 1 Introduction

Heavy-quark production at fixed-target energies provides information and lessons across a range of physics topics. These topics are not so much related to the nature of heavy quarks as such, but rather to our understanding of basic QCD theory, both perturbative and non-perturbative, and to measurements of the nature of hadrons. The results of fixed-target experiments are also necessary to interpret the results of heavy-ion experiments as they search for evidence of quark-gluon plasma. The measurements made by fixed-target experiments can be listed simply enough:

Cross Sections: Total, and as Functions of Beam Energy and Species,  
 $x_F$ , and  $p_t$   
Dependence of Production on Nuclear Target A Value  
Final State Ratios, Particle/Antiparticle Ratios  
Polarization  
Correlations Among Heavy-Quark Particles in the Final State

Each of these measurements relates to one or more of the physics topics. However, the greatest understanding will come from combining multiple measurements, and by ensuring that the parameters used in models are consistent with all the measurements - not just a single measurement at a time. We have not yet really entered the time when this has been done for fixed-target measurements. The closest we come is when perturbative QCD calculations and Monte Carlo simulations with default parameters are compared to data. However, the default parameters have yet to be tuned across the bulk of modern measurements.

## 2 Today's Relevant Experiments and Results for This Meeting

The most relevant fixed-target experiments for the physics topics of interest are listed in Table 1. These experiments cover a variety of beam particle types at a range of energies, and use a plethora of target materials. Fortunately, many production measurements are little affected by the details of target nucleus, and we have learned how to relate measurements on different nuclear targets, at least for inclusive cross sections. Measurements such as production asym-

Table 1: *Current Fixed-Target Heavy-Quark Experiments of Relevance*

Experiment	Beam Momentum (GeV/c)	Beam Particle	Target Material
E690	800	$p$	$LH_2$
E771	800	$p$	Si
E866/NuSea, E789 and E772	800	$p$	$LH_2, LD_2$ , C, Ca, Fe, W Ag, Au, and Cu dump
E769	250	$\pi^\pm, K^\pm$ , and $p$	Be, Al, Cu, and W
E781/SELEX	600	$\Sigma^-$ and $\pi^-$	C and Cu
	572	$p$	C and Cu
E791	500	$\pi^-$	C and Pt
E815/NuTeV	20 to 400	$\nu_\mu, \bar{\nu}_\mu$	Fe
E687	220	$\gamma$	Be
E831/FOCUS	170	$\gamma$	BeO and Si
WA89	340	$\Sigma^-$ and $\pi^-$	C and Cu
WA82	340	$\pi^-$	Si, Cu, and W
	370	$p$	Si and W
WA92/Beatrice	350	$\pi^-$	Cu and W

metries, which are self normalizing, have yet to show target dependences, for example. And, the total charm cross-section measurements on nuclei appear to scale with the number of nucleons in the target nucleus. 1, 2, 3) However, in specific kinematic regions, and for the small fraction of charm production which is “onium,” the A-dependence is more complicated. 4, 5) See the discussion below for this latter effect.

Several measurements are newly available for this conference, and others have only just been published or submitted for publication. These recent and new results are listed by experiment in Table 2. The various results just beginning to appear from FOCUS, SELEX, and NuTeV from the 1996-7 Fermilab fixed-target run bode well for continuing, and even more interesting results in the near future. Nevertheless, it is a good time to review what we have learned so far from the heavy-quark fixed-target experiments of the past.

Table 2: *New Heavy-Quark Production Results for This Conference*

Experiment	Measurement
E690	Diffraction Production of $D^*$
E771	$c$ and $b$ Production by Protons
E791	$D^*$ Production: $x_F, p_t^2$ , Polarization, Asymmetry
E791	$\Lambda_c$ Production Polarization and Asymmetry
E781/SELEX	Production Asymmetries
E831/FOCUS	Charm Particle Correlations
E815/NuTeV	Neutrino Production of Charm
E866	$J/\psi, \psi'$ , and $\Upsilon$ Production and A-Dependence

### 3 Heavy-Quark Production Mechanisms and Measurements

Heavy-quark production is interesting for two reasons. First, the lifetime and uniqueness of the flavor of heavy quarks allows us to follow the progress of a single quark from its production to its emergence as a fully developed hadron observable in the laboratory. Thus, we can probe the time development of hadronic processes involving heavy quarks. Secondly, since the production of heavy quarks by photons and hadrons is so dominated by the gluon content of projectiles (via photon-gluon fusion in photoproduction and gluon-gluon fusion in hadroproduction), the study of heavy-quark production allows the investigation of the gluon content of incident hadrons, both the mesons and baryons in beams and the nucleons in targets. In the case of neutrino interactions, the production of charm is dominated by  $W$ -exchange off strange quarks in the nuclear sea. Thus, we can also learn about strange sea quark distributions in nucleons. In addition, charm production in neutrino Deep Inelastic Scattering is an important ingredient in tests of two-scale perturbative QCD, the two scales being the charm mass and  $\Lambda_{QCD}$ .

We have implicitly assumed that the production process can be divided into separate considerations of the incident partons, their inelastic interaction producing heavy quarks, and the hadronization process of these quarks. This division is referred to as factorization. In the following discussion, each observation will be relevant to one part of the factorized process.

In heavy quark production at fixed-target energies, a single process tends to dominate. For charm quark production, these processes are neutrino-strange-

quark charged current scattering, photon-gluon fusion, and gluon-gluon fusion, respectively for incident neutrinos, photons, and hadrons. In each case, the target parton density plays a direct role, and measurements of each process is sensitive to that parton density. Thus, the strange quark sea distribution can be measured in neutrino charm production, and gluon densities in photo- and hadroproduction of charm.

In neutrino production of charm, E815/NuTeV is just now starting to show results on sea-quark distributions. They have found that the strange and non-strange sea quark distributions have a small asymmetry at most, and that the strange sea is about 40% of the non-strange sea. These results are discussed in more detail in the talk of Maxim Goncharov at this Workshop.

From E769, we have rather direct evidence that the gluon densities in mesons are harder (i.e., have higher momentum fractions on average) than those in nucleons.<sup>6)</sup> This harder gluon momentum leads to more forward production of D mesons when the incident particle is a meson than when it is a proton, as shown in Fig. 1. Note that the pion and kaon appear to produce the same charm particle  $x_F$  distribution, implying that the gluons in pions and kaons are the same, i.e., SU(3) symmetric. This is the same sort of kinematic argument which explains why the photoproduced charm particles are even more forward. The photon interacts with its entire momentum, pushing the subprocess center of mass more forward than typical partons in hadrons, where only a fraction of the hadron momentum goes to each parton.

In the intrinsic charm model of Stan Brodsky, Romona Vogt, and collaborators, a virtual charm quark-antiquark pair appears among the sea quarks of a hadron, and is knocked onto the mass shell during an interaction.<sup>7)</sup> The diagram for this process is explicitly included in higher order perturbation theory. What is different in this model is that the process is pulled out explicitly for calculation, with the initial charm sea quarks given by a parton distribution function. The intrinsic charm was thought to account for 1 to 2% of the proton, an amount required to explain early CERN Intersecting Storage Ring experiment results. These intrinsic charm pairs tend to be co-moving with the valence quarks of their parents. So, it is easy for such quarks to coalesce with valence quarks. This coalescence causes the same asymmetry as would be expected for any other coalescence process; i.e., it should appear at high  $x_F$ . However, we would also expect it to be limited to low  $p_t$ . The evidence is that production

asymmetries are rather flat in  $p_t$ ; 8, 9, 10) so no direct evidence for intrinsic charm exists here. In addition, the differential cross section for  $J/\psi$  production also limits the size of intrinsic charm, to less than 1% *of the prediction* for their Be target. <sup>11)</sup> An earlier measurement in 800 GeV/c proton-Si interactions by E653 <sup>12)</sup> were interpreted as giving a 0.2% upper limit on the amount of intrinsic charm in the proton.

#### 4 Cross Sections

The total charm cross section (typically taken as dominated by the inclusive ground-state meson production cross section) has been measured in photoproduction and hadroproduction over energies from about ten GeV to hundreds of GeV. Cross sections have also been calculated in leading order (LO) and next-to-leading order (NLO) in perturbative QCD. The ratio of NLO to LO cross sections is sometimes referred to as the “K-factor.” This factor is significantly greater than one, typically a factor of a few. Nevertheless, it is considered likely that next-to-next-to-leading order terms will not be so important. The NLO differential cross sections, like the total cross sections, appear to be related to the LO calculations by more-or-less a single number, the same K-factor. So, shapes of distributions do not change much, and the absolute values are usually played down compared to relative differential cross sections (shapes).

The range of fixed-target photoproduction results are extended to 40 TeV equivalent photon beam energy by measurements at the HERA collider. Even these highest-energy photoproduction data fit a NLO calculation over the full range quite well. <sup>13)</sup> Note, however to watch the inclusion of color-octet effects at low photon energy and the parameters used in the cited calculation. Even so, the theoretical uncertainties in photoproduction are rather smaller than those for hadroproduction, where uncertainties associated with the charm-quark mass and the appropriate scale for the calculations each give uncertainties of nearly an order of magnitude. The pattern of cross-section measurements agree with each other across the full range of experiments and energies quite well. <sup>14)</sup>

The total beauty cross section at fixed-target experiments has been measured at various energies for both incident pions and protons. The measurements usually come from incomplete B decay observations; e.g.,  $J/\psi$ 's which do not come from the primary interaction, and are presumed to be from B decays. <sup>15)</sup> The data exists for incident pions and protons, and is quite consis-

tent with the exception of one measurement with incident 800 GeV/ $c$  protons. Unfortunately, even for the heavy bottom quark, the NLO QCD calculations have an uncertainty of a factor of nearly ten.

It is worth noting explicitly that all the heavy-quark-production calculations use a universal running value of  $\alpha_S$ . Any discrepancy between comparisons of calculations of charm and bottom data could have been evidence for a breakdown of QCD. However, in this context it is worth noting the limits on such non-universality of the strong coupling are severely limited by measurements from  $e^+e^-$  collisions.<sup>16)</sup>

Another production topic of interest is the size of diffractive charm production. In the old days, several CERN and Fermilab experiments tried to see charm in diffractive events. It was hoped that this process would be quite large, perhaps 10% of the total charm photoproduction, for example. Now, we have a first measurement of the process, but for incident protons, from E690. The experiment triggers on a fast, forward proton and looks for  $D^*$  mesons (See Fig. 2.). Their measurement of the total diffractive  $D^*$  production cross section is model dependent, ranging from 0.17 to 0.29 mb ( $\pm 0.05$  mb statistical error). The total charm diffraction is, thus, about 0.75 mb, only about 2 % of the total charm cross section. No wonder the early experiments requiring large diffractive charm production saw so few charm decays.

The charmonium cross sections are a real mystery, both at fixed-target energies and at the Tevatron Collider. There is data on  $J/\psi$ ,  $\psi'$ ,  $\Upsilon$ ,  $\chi_1$ , and  $\chi_2$ . The well-publicized, but unexplained large Collider direct  $J/\psi$  and  $\psi'$  production (6x and 25x greater than LO calculations, respectively - really large K-factors!) occurs also at fixed-target energies, and is shown from E789 in Fig. 3 where the production is 7x and 25x larger, respectively, than the LO calculations!<sup>17)</sup> Can the fixed-target  $\chi_1$  and  $\chi_2$  production shed light on this?

There are three production models considered in the literature. Each makes a prediction on the relative  $\chi_1$  and  $\chi_2$  production in  $pN$  interactions. The three models, and their predictions are:

Color singlet –  $\chi_1 \sim 5\%$  of  $\chi_2$  production.

Color evaporation/color bleaching –  $\chi_1:\chi_2$  production 3:5.

Non-Relativistic QCD (color octet plus color singlet) –  $\chi_1$   
up to 30% of  $\chi_2$  production.

The inclusion of color-octet processes seems to explain the observations in hadroproduction.<sup>18)</sup> Yet, the color-octet matrix elements from the Tevatron don't work at HERA. Further complicating the situation is that the expected polarization of color-octet produced charmonium seems not to be present at the Tevatron Collider!<sup>19)</sup>

Some of the most beautiful data of recent years comes from the series of experiments in Fermilab's Meson East beam line. Very high statistics measurements of dimuon production give impressive signals for Drell-Yan pairs and the heavy-quark onia states as well.<sup>4, 11, 20)</sup> Among their results is a study of the  $A$ -dependence of open charm<sup>1)</sup> (which agrees with the  $A^1$  results of others) and of  $J/\psi$  and  $\psi'$  (which are of higher detail and precision).

As shown in Fig. 4, the  $A$ -dependence for  $J/\psi$  and  $\psi'$  production is not simple, varying by kinematic region, though quite similar for  $J/\psi$  and  $\psi'$ . Are the details of the  $x_F$  and  $p_t$  dependences evidence for color-octet production? Another feature of these data is the cautionary note sounded against too easy interpretation of  $J/\psi$  production effects in heavy-ion collisions as evidence for quark-gluon plasma. The data shown in Fig. 4 demonstrate that using a single power  $\alpha$  in predictions cannot be a complete model. In fact, who is to say that the dense nuclear matter does not mix the kinematic regions we think of from fixed-target measurements. What values of  $\alpha$  are relevant?

In these discussions of cross sections, we have an example of the need to subject model calculations to the full range of observations before anointing any model. So far, this has only been done piecemeal, and no model seems to explain all the observations.

## 5 Hadronization/Fragmentation

In the factorization scheme, the final stage involves turning the produced heavy quarks into the hadrons seen in the laboratory. This process is usually referred to variously as fragmentation and hadronization. The term fragmentation carries with it an implication of independence of the heavy quark and antiquark in the process, and the use of "fragmentation functions" measured in  $e^+e^-$  collisions. However, the environments of hadronic collisions and of  $e^+e^-$  collisions are quite different in terms of the totality of color fields present. We will see that this difference is quite evident, and the term hadronization appropriately



conveys a more complex situation.

Longitudinal momentum distributions of heavy-quark particles are usually presented as functions of the scaled variable, Feynman  $x$ ,  $x_F$ . This scaling is relative to the maximum kinematically allowed value, meaning that the variable runs from  $-1.0$  in the backward direction to  $+1.0$  in the forward direction. Plotting distributions versus  $x_F$  makes the distributions measured at various energies look about the same. More interestingly, and as shown in Fig. 5, the observed  $D$  meson  $x_F$  distributions look like the QCD predictions for quarks.<sup>14)</sup> The  $x_F$  distribution does not look like the prediction for mesons when fragmentation functions are used to go from quarks to hadrons.

Why should observed hadrons appear to have more momentum than you might expect after fragmentation? There must be some process other than simple fragmentation which contributes forward momentum to balance what would be lost by fragmentation. Such a process has been called “color drag.” It refers to the color string attachment between the produced heavy quarks and the remnant quarks of projectiles. The forward-moving remnants “pull” the heavy quark forward during the hadronization process. As we will see below, production asymmetries lend credence to this idea.

In hadroproduction, the longitudinal distributions of heavy-quark particles and antiparticles may differ even though the leading order QCD process is symmetric in quark and antiquark production. In fact, even including next-to-leading order processes only produces a very small asymmetry in the far forward direction. What is observed in experiments, for example, is large asymmetries when a heavy-quark particle has a valence light-quark in common with the incident hadron and the antiparticle does not.<sup>8, 9, 10, 21)</sup> This is known as the “leading particle effect.” Of course, it should also refer to asymmetries in the backward direction when heavy-quark particles have light valence-quarks in common with the target hadrons.

The effect is understood as being due to the coalescence of the heavy quark with a valence quark from projectile (or target) when the heavy quark and light quark are close in phase space. The experimental evidence supports this picture across a wide variety of charm particles and incident beam particle types.

There are also particle/antiparticle asymmetries in photoproduction. In the photon direction, or centrally, the process must have another explana-

tion. There, we may be seeing the effects of associated production (meson with baryon). The energy threshold for such associated production is less than for heavy baryon-antibaryon production. And, we may expect that this associated production effect is also responsible for some of the asymmetry seen in hadroproduction, especially in the central region (near  $x_F$  of zero).

The coalescence/recombination model seems to provide a framework for understanding particle/antiparticle production asymmetries. Intrinsic charm is not apparently required. Leading-particle effects increase in the forward and backward directions, according to the expectations tied to valence-quark content.

A particularly interesting feature of the asymmetries is that they are more or less flat in  $p_t$ .<sup>8, 9, 10, 21)</sup> This feature appears in the PYTHIA/JETSET simulations, but is not expected in the intrinsic quark model as suggested above. It should be noted, however, that the default parameters of current versions of the PYTHIA/JETSET software do not get the details of the  $x_F$  and  $p_t$  asymmetry dependences right (see below).

Experimenters typically report particular measurements in their papers, rather than presenting more universal coverage of results, even their own. When making comparisons, they may vary the input parameters of models to find those that provide the best match to the particular measurement being presented. E791, for example, in comparing their  $D^\pm$  production asymmetry to PYTHIA predictions, show both the default parameter predictions and those with modified parameters.<sup>10)</sup> In particular, the charm quark mass and intrinsic  $k_t$  (see discussion of this parameter below) are changed from 1.35 GeV/ $c^2$  and 0.44 GeV/ $c$  to 1.7 GeV/ $c^2$  and 1.0 GeV/ $c$ . The paper notes that these parameters are not unique in obtaining agreement, and that it is necessary to select a set of parameters which fit this and a range of other measurements to have any confidence in the parameters.

We are just starting to see detailed measurements of the production polarization of heavy-quark particles. Previously,<sup>22)</sup> data on the heavy-quark particles which carry spin have not been sufficiently copious to allow such determinations. Now, E791 has measured polarization for the open-charm  $D^*$  and  $\Lambda_c$  particles. For the  $D^*$ , they now have the spin-density matrix elements as functions of  $x_F$  and  $p_t^2$  as shown in Fig. 6. For the  $\Lambda_c$ , the full E791 decay analysis includes the  $\Lambda_c$  polarization as a function of  $p_t$ .<sup>23)</sup>

Onium production polarization is also measured, and is useful in determining the extent of color-octet contributions to the production cross section. Models of color-octet production predict large polarization. Yet, E866/NuSea observes little polarization for the onium ground states, and quite large polarizations for the excited onium states. <sup>24)</sup>

The simplest models of heavy-quark production predict that the heavy-quark particle and antiparticle will appear back-to-back in the center of mass. This correlation carries over directly to the laboratory angle in the transverse plane between the particle and antiparticle. It is the simplest correlation to measure, requiring less than complete reconstruction of the particle and antiparticle.

The earliest observations of particle/antiparticle correlations were made with the complete reconstruction of one charm particle, and incomplete reconstruction of the mate. Now, E791 and FOCUS have made high statistics measurements with the complete reconstruction of both particles (Fig. 7), reducing the uncertainties associated with acceptance corrections on the second particle. A broad range of correlations has been published by E791. <sup>25)</sup>

Given time constraints, I will only discuss one correlation. This one leads to the distribution in the angle between the charm particle and antiparticle in plane transverse to the beam. The E831/FOCUS photoproduction data (like earlier, lower statistics measurements) is much more peaked at 180 degrees (the back-to-back angle) than the E791 hadroproduction data (Fig. 7). Thus, the hadronic environment plays a critical role in smearing the simpler QCD predictions of perturbative calculations and parton-shower simulations.

## 6 Intrinsic $k_t$

All the transverse momentum distributions in LO calculations tend to be unphysical delta-functions, like the back-to-back production discussed above. NLO and parton shower models provide smearing due to gluon emission, etc. However, this smearing is not enough to match the measured distributions like those for  $p_t$  and the transverse angle between the particle and antiparticle. <sup>25)</sup> Several simulation packages insert an additional effect, that due to transverse momentum of initial partons in hadrons. This transverse momentum is called “intrinsic  $k_t$ .”

When the model intrinsic  $k_t$  is varied until the simulation predictions

match data, we find that  $k_t$  in the range of 1 to 3 GeV/ $c$  is needed. How can the intrinsic  $k_t$  of partons inside a proton or neutron be typically much more than the nucleon rest mass? Intrinsic  $k_t$  must be a misnomer for something else. But, what?

## 7 Concluding Remarks

In this review, we have seen a large amount of quality, fixed-target, heavy-quark production data. There is still more to come: from FOCUS, SELEX, and COMPASS. Each of the present experiments is providing a healthy variety of observations.

The major features of our understanding of this heavy-quark production data are (1) factorization of the process, (2) the perturbative-QCD production of the heavy quarks - dominated by gluons in the incident hadrons, and (3) a more-or-less complicated hadronization. The picture works fairly well in describing the data. Nevertheless, there are also, still, several outstanding issues. I would mention particularly:

Understanding the K-factor for charm and beauty production, including any role of the color-octet process.

Understanding the onium cross sections and the role, if any, of the color-octet process.

Untangling intrinsic  $k_t$ , and seeing it as shorthand for ... what?

Being better able to understand the relation between A-dependence effects in fixed-target experiments and the quark-gluon plasma signatures sought in heavy-ion collisions.

We can benefit from detailed, systematic comparisons across the range of observations made, particularly comparing open and hidden heavy flavor mesons, comparing mesons and baryons, and comparing the varied spin states and particle types (i.e., with varied light valence quarks in the final heavy-quark particle). In addition, we must have parameter sets which explain the full range of observations, not just parameters which are tuned measurement-by-measurement.

Achieving a more complete understanding of the production of heavy quarks, even at fixed-target energies, will help us understand QCD itself, as

well as help to provide guidance in our studies of the signals and backgrounds for the even heavier objects to come at the highest energies.

## 8 Acknowledgements

I would like to give special thanks to Chuck Brown (NuSea), Dave Christian (E690), Peter Cooper (SELEX), Brad Cox (E771), Erik Gottschalk (E690 and FOCUS), David Langs (E791), Jim Russ (SELEX), and Panagiotis Spentzouris (E815) for help obtaining the latest results. I also want to thank the organizers of the very useful and enjoyable HQ2K meeting.

## 9 Comments and Questions From Attendees

Comment from Brad Cox:

“Let me emphasize one point you made. Those people who are doing heavy ion collisions should take into account the complex A dependences seen in many fixed-target experiments. Only then will the observations that they make be on solid ground.”

Question from Ikaros Bigi:

“You showed very intriguing data from E791 on the polarization of  $\Lambda_c$  produced by pions. Can one conjecture then that FOCUS and SELEX will have sizable samples of polarized  $\Lambda_c$  and  $\Xi_c$ ?”

Reply from Appel:

“Yes, I hope that we will see results from such samples. Of course, the polarization may be quite different with incident photon and hyperon beams. That’s part of the interest these results should have.”

## References

1. E789 Collaboration, M.J. Leitch *et al.*, Phys. Rev. Lett. **72**, 2542 (1994);
2. E769 Collaboration, G.A. Alves *et al.*, Phys. Rev. Lett. **70**, 722 (1993).
3. WA82 Collaboration, M. Adamovich *et al.*, Phys. Lett. B **284** 453 (1992).

4. E866/NuSea Collaboration, R.E. Tribble *et al.*, Nucl. Phys. A **663** 761 (2000); E789 Collaboration, M.J. Leitch *et al.*, Phys. Rev. D **52** 4251 (1995);
5. E772 Collaboration, D.M. Alde *et al.*, Phys. Rev. Lett. **66** 2285 (1991).
6. E769 Collaboration, G.A. Alves *et al.*, Phys. Rev. Lett. **77**, 2392 (1996).
7. R. Vogt and S.J. Brodsky, Nucl. Phys. B **478**, 311 (1996); S.J. Brodsky *et al.*, Phys. Lett. B **93**, 451 (1980).
8. E769 Collaboration, G.A. Alves *et al.*, Phys. Rev. Lett. **72**, 812 (1994); Erratum-ibid. **72**, 1946 (1994).
9. E791 Collaboration, E.M. Aitala *et al.*, Phys. Lett. B **411**, 230 (1997).
10. E791 Collaboration, E.M. Aitala *et al.*, Phys. Lett. B **371**, 157 (1996).
11. E789 Collaboration M.S. Kowitt *et al.*, Phys. Rev. Lett. **72**, 1318 (1994).
12. E653 Collaboration K. Kodama *et al.*, Phys. Lett. B **316**, 188 (1993).
13. A.V. Berezhnoy, V.V. Kiselev, and A.K. Likhoded, hep-ph/9905555.
14. E791 Collaboration, E.M. Aitala *et al.*, Phys. Lett. B **462**, 225 (1999).
15. E771 Collaboration, T. Alexopoulos *et al.*, Phys. Rev. Lett. **82**, 41 (2000).
16. SLD Collaboration, K. Abe *et al.*, Phys. Rev. D **59**, 012002 (1999).
17. E789 Collaboration M.H. Schub *et al.*, Phys. Rev. D **52**, 1307 (1995).
18. E771 Collaboration, T. Alexopoulos *et al.*, Phys. Rev. D **62**, 032006 (2000).
19. CDF Collaboration, T. Affolder *et al.*, Phys. Rev. Lett. **85**, 2886 (2000).
20. E866 Collaboration, M.J. Leitch *et al.*, Phys. Rev. Lett. **84**, 3256 (2000).
21. E781/SELEX Collaboration, M. Iori *et al.*, hep-ex/9910039.
22. M. Jezabek, K. Rybicki, and R. Rylko, Phys. Lett. B **286**, 175 (1992).
23. E791 Collaboration, E.M. Aitala *et al.*, Phys. Lett. B **471**, 449 (2000).
24. E866/NuSea Collaboration, C.N. Brown *et al.*, hep-ex/0011030.
25. E791 Collaboration, E.M. Aitala *et al.*, EPJdirect C **4**, 1 (1999).

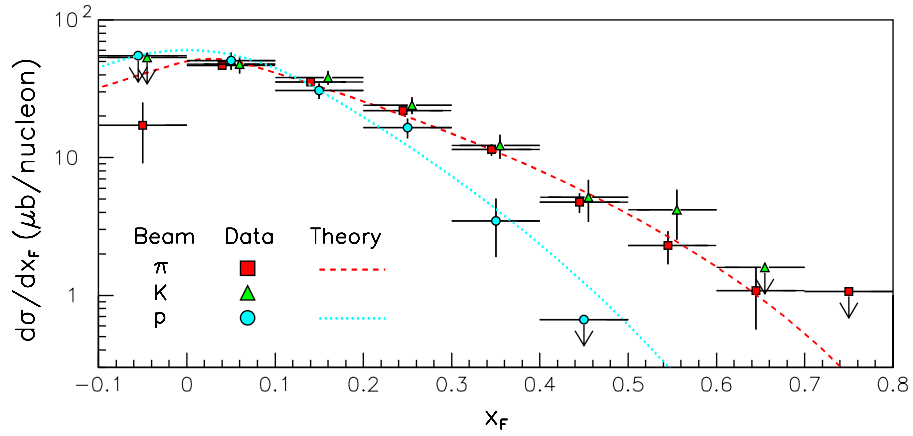


Figure 1: *E769* inclusive charm particle  $x_F$  distributions showing  $\pi$  and  $K$  meson beams leading to similar results, different from those for incident protons.

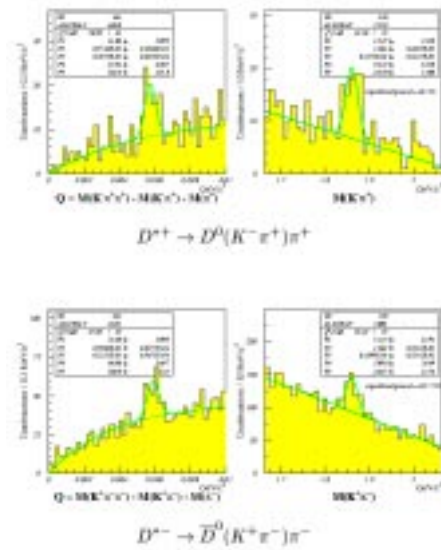


Figure 2: *E690* diffractive  $D^*$  signals, using the usual decay to  $D^0 \pi$ . The data come from  $p p \rightarrow p_{forward} D^* X$  with  $x_{F,p_{forward}} > 0.85$ . The  $D^{*+}$  signal is on top,  $D^{*-}$  on the bottom. The decay  $Q$ -value is shown on the left for the  $D^0$  mass-peak regions on the right.

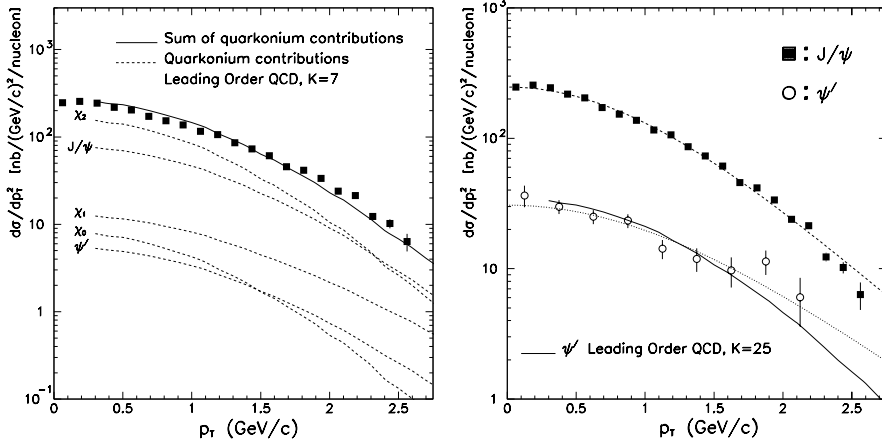


Figure 3: *E789 data on  $J/\psi$  and  $\psi'$  production cross sections and NLO calculations times large  $K$  factors chosen to match the data.*

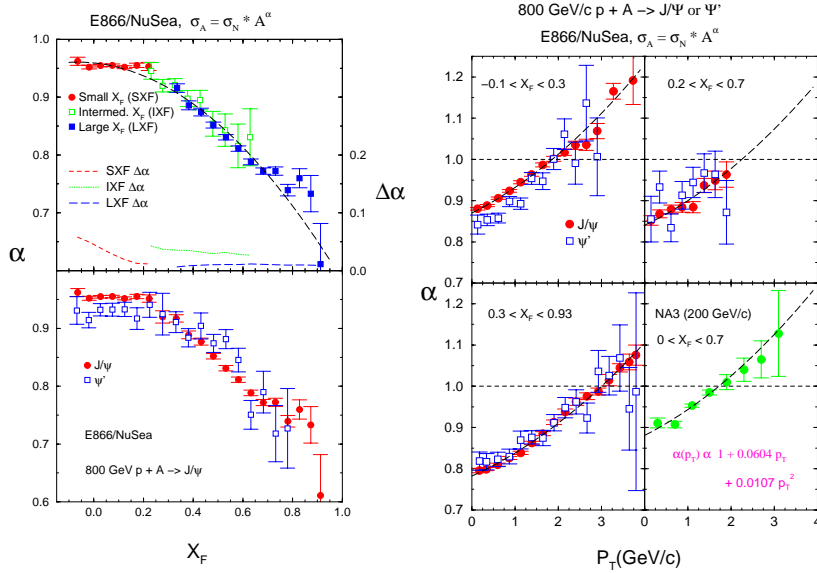


Figure 4: *E866 data on  $J/\psi$  and  $\psi'$  production  $A$ -dependence showing rather nonuniform values of  $\alpha$ , the power of  $A$  in the cross section.*



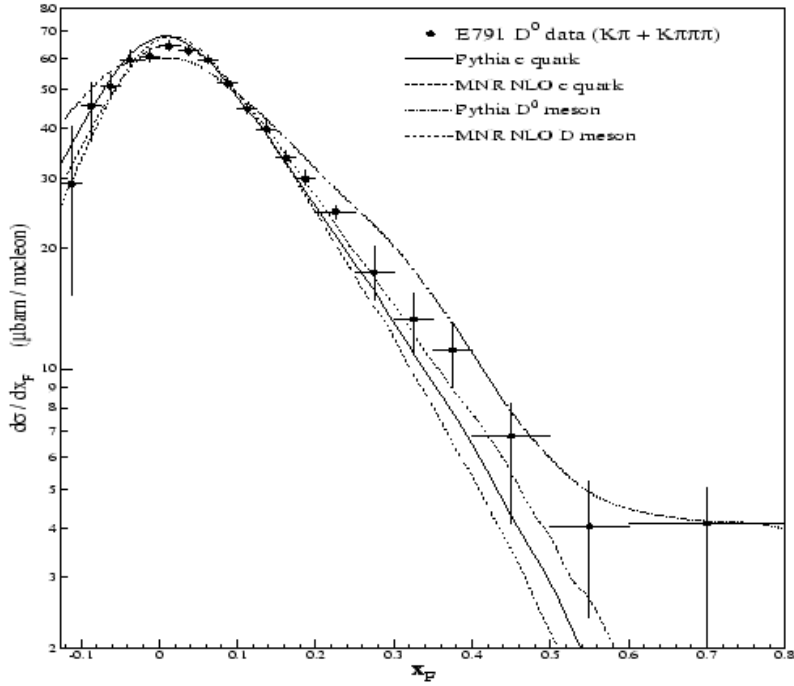


Figure 5: *E791 inclusive  $D^0$  production  $x_F$  distribution. The meson data match the predictions for quarks better than that for mesons.*

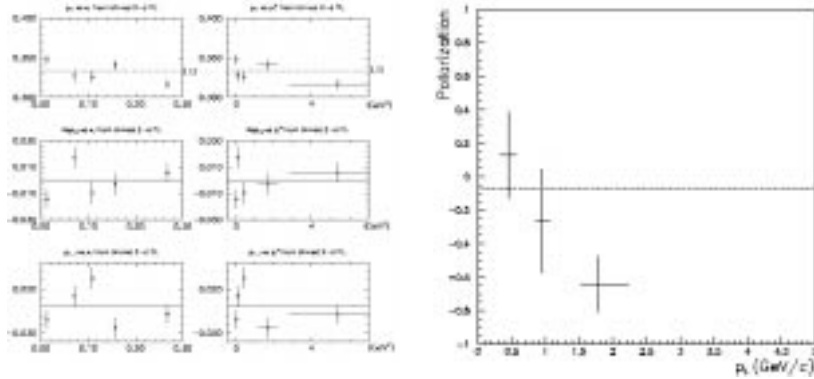


Figure 6: *E791  $D^*$  spin-density matrix elements vs  $x_F$  and  $p_t$  (left) and  $\Lambda_c$  polarization vs  $p_t$  (right).*

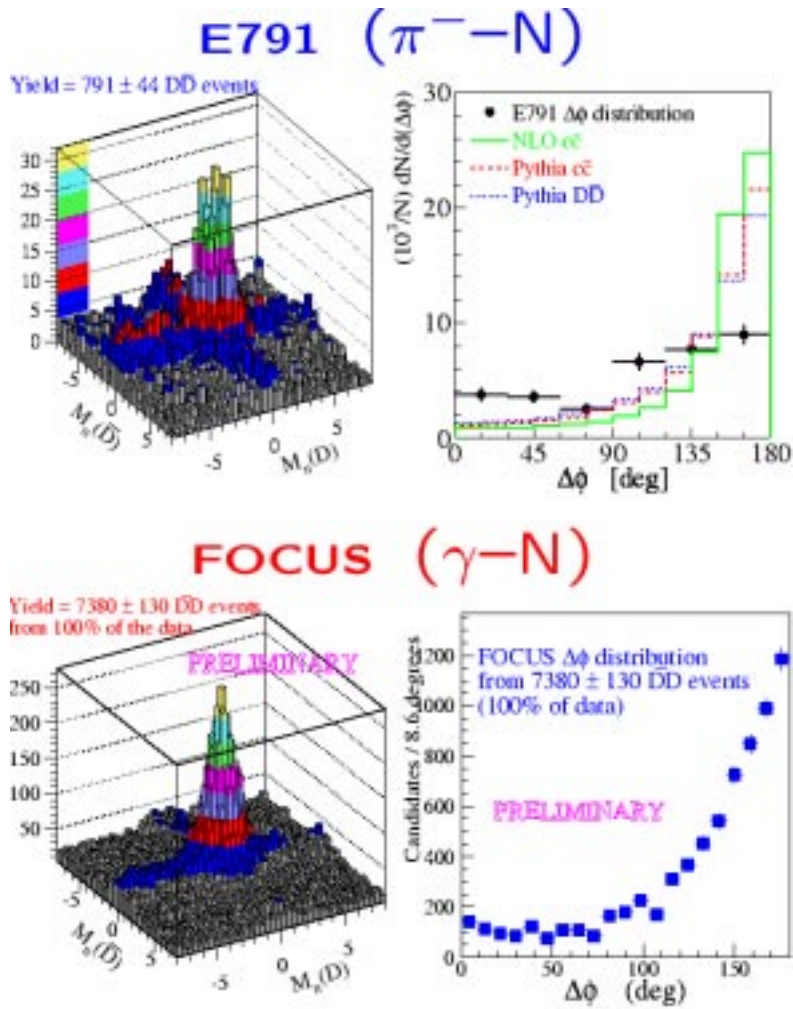


Figure 7: Comparison of charm photoproduction (E831/FOCUS) and hadroproduction (E791) particle-antiparticle correlations in the plane transverse to the incident beam.